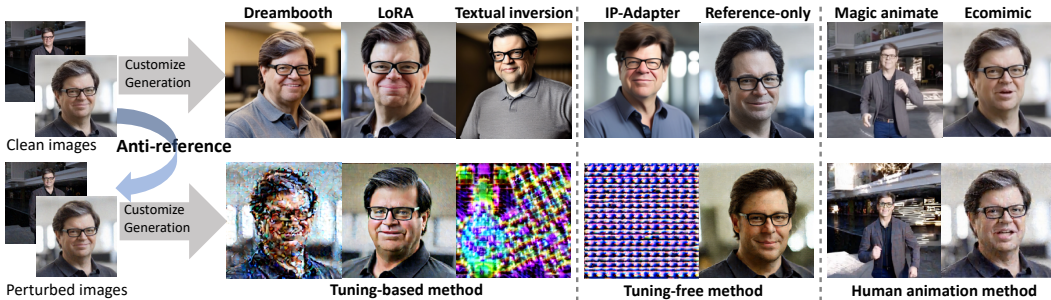


# 000 001 002 003 004 005 006 007 008 009 010 011 012 013 014 015 016 ANTI-REFERENCE: UNIVERSAL AND IMMEDIATE DE- FENSE AGAINST REFERENCE-BASED GENERATION

005 **Anonymous authors**

006 Paper under double-blind review



017 Figure 1: Malicious attackers can collect users’ images as reference images and use diffusion models  
018 to achieve malicious purposes. Our system, called Anti-reference, applies imperceptible perturbations  
019 to user-uploaded images before they are published, resulting in noticeable artifacts in images or  
020 videos generated by reference-based methods and fine-tuning approaches. This makes it easy to  
021 recognize them as AI-generated, thus protecting the images.

## 022 ABSTRACT

024 Diffusion models have revolutionized generative modeling with their exceptional  
025 ability to produce high-fidelity images. However, misuse of such potent tools  
026 can lead to the creation of fake news or disturbing content targeting individuals,  
027 resulting in significant social harm. In this paper, we introduce Anti-Reference,  
028 a novel method that protects images from the threats posed by reference-based  
029 generation techniques by adding imperceptible adversarial noise to the images.  
030 We propose a unified loss function that enables joint attacks on fine-tuning-based  
031 customization methods, non-fine-tuning customization methods, and human-centric  
032 driving methods. Based on this loss, we train a Adversarial Noise Encoder to predict  
033 the noise or directly optimize the noise using the PGD method. Our method shows  
034 certain transfer attack capabilities, effectively challenging both gray-box models  
035 and some commercial APIs. Extensive experiments validate the performance of  
036 Anti-Reference, establishing a new benchmark in image security.

## 038 1 INTRODUCTION

039 Customized diffusion models can be divided into methods that require training, Ruiz et al. (2023);  
040 Hu et al. (2021); Gal et al. (2022); Kumari et al. (2023) and those that do not, such as IP-Adapter  
041 (Ye et al., 2023a), Instant-ID (Wang et al., 2024b). Reference-based methods are widely used in  
042 customized image and video generation, especially in human-centered video generation, including  
043 portrait video creation methods(Tian et al., 2024; Chen et al., 2024; He et al., 2024; Xie et al., 2024),  
044 and human animation (Xu et al., 2024; Hu, 2024) , which have attracted significant attention due to  
045 their practical value in creating digital human avatars and enhancing film production.

046 Reference-based methods that require no training offer high convenience and efficiency, but when  
047 misused, they can have severe negative social impacts, such as creating fake news or pornographic  
048 images targeting individual victims. Existing studies use encoder attack (Salman et al., 2023) and  
049 diffusion attack (Van Le et al., 2023; Liang et al., 2023) to protect images from the threats posed by  
050 methods requiring fine-tuning, using PGD (Madry, 2017) optimization to generate adversarial noise,  
051 but this approach requires several minutes to protect a single image, severely limiting its practical  
052 application. Moreover, these methods are largely ineffective against non-trainable Reference-based  
053 generation methods. Therefore, developing an efficient method to protect personal images from the  
threats of Reference-based generation has become an urgent priority.

054 Reference-based methods provide additional conditions through a Reference Image to enable cus-  
 055 tomized generation. These methods can be divided into two types based on their implementation: one  
 056 type embeds Reference features in the cross-attention layer of the denoising network using an adapter,  
 057 such as IP-Adapter (Ye et al., 2023a); the other type embeds reference features in the self-attention  
 058 layer of the denoising network using ReferenceNet. The approach of ReferenceNet is widely used  
 059 for image customization generation (Team, 2023; Zhang et al., 2024b;c), Image2Video (Chen et al.,  
 060 2023; Zhang et al., 2023), and face animation generation (Tian et al., 2024; Chen et al., 2024; He  
 061 et al., 2024; Xie et al., 2024), and body-driven tasks (Xu et al., 2024; Hu, 2024). However, due to  
 062 the variety of existing Reference-based generation methods, attacking a specific method has limited  
 063 practical significance, as attackers can easily switch methods to bypass protection. Therefore, the  
 064 motivation of this paper is to propose a universal adversarial noise generation method to address the  
 065 threats posed by mainstream Reference-based methods.  
 066

066 In practical image protection scenarios, protection methods need to address several challenges. Firstly,  
 067 universality is a key challenge. Since Reference-based methods have many different implementations,  
 068 and models trained on different datasets have different feature spaces, the same attack strategy  
 069 may have very different effects on different models. Secondly, efficiency is also crucial. Existing  
 070 methods like Anti-DreamBooth (Van Le et al., 2023) , which use PGD optimization, usually require  
 071 hundreds of steps and significant time, severely limiting their feasibility for real-time applications.  
 072 Finally, black-box or gray-box transferability and robustness are also central challenges. In practical  
 073 applications, the structures and parameters of proprietary APIs like EMO (Tian et al., 2024) , Animate  
 074 anyone (Hu, 2024) are not accessible, so attack methods must have good gray-box transferability.  
 075 Additionally, the generated adversarial noise also needs to be robust enough to withstand common  
 076 data augmentation operations and preprocessing steps.  
 077

077 To address these challenges, this paper presents Anti-Reference, the first to protect images from  
 078 the threats posed by mainstream reference-based methods and tuning-based customization methods  
 079 through the forward process. We propose a Noise Encoder based on the ViT (Dosovitskiy, 2020)  
 080 architecture, which predicts adversarial noise of the same size as the original image and overlays it to  
 081 form a protected image. To achieve a universal attack on methods requiring fine-tuning and those  
 082 that do not, we designed a unified loss function, using a weighted strategy to achieve joint attack  
 083 effects across multiple tasks, and by limiting the noise range and regularization loss to ensure the  
 084 invisibility of the noise. To enhance the robustness of adversarial noise, we also introduced some data  
 085 augmentation techniques to ensure that the adversarial noise can withstand various data enhancements  
 086 and preprocessing operations. As the model structures and weights of proprietary APIs are not  
 087 accessible, directly attacking these models is usually not feasible. To overcome this hurdle, we created  
 088 white-box proxy models that mimic the structure and behavior of these proprietary models, and we  
 089 successfully implemented attacks on these proxy models, thereby achieving gray-box transferability  
 090 attacks. Specifically, our adversarial samples have successfully transferred to closed-source APIs  
 091 (such as Animate Anyone (Hu, 2024) and EMO (Tian et al., 2024)). Extensive experimental results  
 092 demonstrate that Anti-Reference is highly effective in protecting images from potential security  
 093 threats posed by reference-based generation methods and fine-tuning-based approaches.  
 094

094 We summarize our main contributions as follows:  
 095

- 095 • We introduce a universal method for attacking customized diffusion models for the first time,  
 096 which is effective against both mainstream reference-based generation methods and those  
 097 requiring fine-tuning.
- 098 • We introduce an Adversarial Noise Encoder that executes attacks without the need for  
 099 traditional PGD optimization, significantly reducing computational time and enhancing  
 100 suitability for real-time applications.
- 101 • We have designed transferable adversarial samples that enable gray-box attacks on com-  
 102 mercial APIs using white-box proxy models. These samples are robust, showing strong  
 103 resistance to common image transformations.

## 104 2 RELATED WORK

### 105 2.1 CUSTMIZED DIFFUSION MODEL.

106 Diffusion probability models Song et al. (2020); Ho et al. (2020) represent a class of advanced gener-  
 107 ative models that reconstruct original data from pure Gaussian noise by learning noise distributions

108 at different levels. These models excel in handling complex data distributions and have marked  
 109 significant accomplishments across various fields such as image synthesis Rombach et al. (2021);  
 110 Peebles & Xie (2023), image editing Brooks et al. (2023); Hertz et al. (2022), video generation Wu  
 111 et al. (2022); Hu (2024), and 3D content creation Poole et al. (2022). A prominent example is Stable  
 112 Diffusion Rombach et al. (2021), which utilizes a UNet architecture to iteratively produce images,  
 113 demonstrating robust text-to-image capabilities after extensive training on large text-image datasets.  
 114 DreamBooth Ruiz et al. (2023), Custom diffusion Kumari et al. (2023) and Textual Inversion Gal  
 115 et al. (2022), adopt transfer learning to text-to-image diffusion models via either fine-tuning all the  
 116 parameters, partial parameters , or introducing and optimizing a word vector for the new concept.  
 117 LoRA (Low-Rank Adaptation) Hu et al. (2021) is a popular and lightweight training technique that  
 118 significantly reduces the number of trainable parameters and is widely used for personalized or  
 119 task-specific image generation.  
 120

## 121 2.2 REFERENCE-BASED GENERATION

122 In addition to the aforementioned fine-tuning methods, finetuning-free customized generation methods  
 123 can capture concepts from a single image and are widely used for tasks such as customized generation  
 124 (Ye et al., 2023a; Mao et al., 2024; Zhang et al., 2024a), identity consistency maintenance (Wang  
 125 et al., 2024b; Li et al., 2024), face-driven Tian et al. (2024); Chen et al. (2024); Xie et al. (2024), and  
 126 body-driven tasks Xu et al. (2024); Hu (2024). These methods can be roughly categorized into the  
 127 Adapter approach and the ReferenceNet approach based on how the reference image features are  
 128 utilized. In the Adapter approach, the reference image is first processed by a pre-trained image feature  
 129 extractor, typically CLIP (Radford et al., 2021) image encoder or ArcFace Deng et al. (2019), and then  
 130 an adapter structure generates visual tokens applied to the cross-attention layers of the U-Net. The  
 131 ReferenceNet approach emphasizes the effectiveness of integrating reference image features into the  
 132 self-attention layers of LDM U-Nets, enabling customized generation while preserving appearance  
 133 context. Image-to-video technology Chen et al. (2023); Zhang et al. (2023) uses ReferenceNet to  
 134 maintain consistency between the generated results and the reference image. Magic Animate Xu  
 135 et al. (2024) and Animate Anyone Hu (2024) combine ReferenceNet with pose control and temporal  
 136 modules to achieve body-driven generation. EMO Tian et al. (2024), Ecomimic Chen et al. (2024),  
 137 and X-Portrait Xie et al. (2024), among other talking-face methods, maintain identity consistency  
 138 using ReferenceNet, generating fake videos from just a single photo. The misuse of Reference-based  
 139 Generation methods can have severe consequences, making it urgent to protect images from the  
 140 threats posed by such methods.

## 141 2.3 PROTECTIVE PERTURBATION AGAINST DIFFUSION.

142 Protecting the security of personal images is of great significance Dong et al. (2023); Qiao et al.  
 143 (2024); Dai et al. (2024) . To protect personal images such as faces and artwork from potential  
 144 infringement when used for fine-tuning Stable Diffusion, recent research aims to disrupt the fine-  
 145 tuning process by adding imperceptible protective noise to these images. Several methods have been  
 146 developed to achieve this goal: Glaze (Shan et al., 2023) focuses on preventing artists' work from  
 147 being used for specific style mimicry in Stable Diffusion. It optimizes the distance between the  
 148 original image and the target image at the feature level, causing Stable Diffusion to learn the wrong  
 149 artistic style. AdvDM (Liang et al., 2023) proposes a direct adversarial attack on Stable Diffusion  
 150 by maximizing the Mean Squared Error loss during the optimization process. This approach uses  
 151 adversarial noise to protect personal images. Anti-DreamBooth (Van Le et al., 2023) incorporates  
 152 the DreamBooth fine-tuning process of Stable Diffusion into its consideration. It designs a bi-level  
 153 min-max optimization process to generate protective perturbations. Additionally,other research efforts  
 154 (Wang et al., 2024a; Ye et al., 2023b; Zheng et al., 2023) have explored generating protective noise  
 155 for images using similar adversarial perturbation methods.

156 The previously mentioned methods utilize adversarial noise to influence the fine-tuning process,  
 157 preventing models from learning from tampered images. These techniques effectively target models  
 158 that require fine-tuning. However, reference-based generation methods do not rely on fine-tuning but  
 159 directly generate images from existing data, making these adversarial protections ineffective against  
 160 them. Effective protection against reference-based generation attacks requires new strategies that  
 161 can directly intervene in the image retrieval and matching mechanisms. Effective protection against  
 reference-based generative attacks requires the development of new strategies.

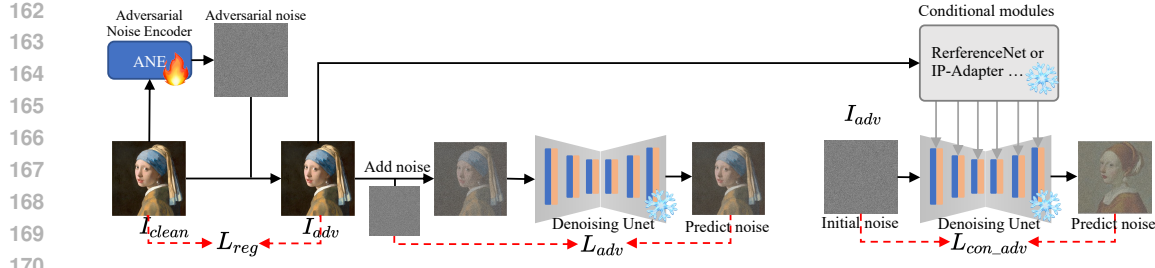


Figure 2: Illustration of Anti-reference. To defend against customized generation attacks, we introduce a loss function that guides the training of a noise encoder to produce adversarial perturbations, effectively protecting source images.

### 3 PROBLEM DEFINITION

Considering the practical implications of image infringement based on Stable Diffusion, it is essential to define the threat model in real-world scenarios. We consider two participants involved in fine-tuning Stable Diffusion using images: the "User" Alice and the "Photo Thief" Bob. Photo Thief Bob illicitly uses reference-based methods to exploit others' photos for customized content, while User Alice, wishing to safeguard her images on social media, adds adversarial noise to disrupt Bob's methods, aiming to induce severe artifacts in the generated content. Specifically, we explain the workflow of the two parties as follows:

**User Alice:** Alice aims to protect her images from exploitation by Stable Diffusion by applying nearly imperceptible protective perturbations, while minimizing alterations to the original images. Her main challenge is the uncertainty of which methods Photo Thief Bob will use to fine-tune these protected images. She also needs to ensure that these protection measures remain effective even when the images undergo natural transformations such as cropping, compression, and blurring during dissemination.

**Photo Thief Bob:** Bob downloads Alice's photos and uses customized generation methods to create inappropriate content. Bob can choose any mainstream fine-tuning method, including but not limited to direct fine-tuning, LoRA, Textual Inversion, DreamBooth, or Custom Diffusion.

The goal of this work is to add imperceptible adversarial noise to images, formalized as  $I_{adv} = I + \text{noise}$ , where  $I$  and  $I_{adv}$  represent the original and protected images, respectively. These images serve as inputs to customization methods, and the outputs  $\text{Gen}(I)$  and  $\text{Gen}(I_{adv})$  are compared. If  $\text{Gen}(I_{adv})$  exhibits significant distortion, the protection is considered successful. We achieve this by solving the following optimization problem:

$$\max_{x_{adv} \in M} d(\text{Gen}(I), \text{Gen}(I_{adv})) \text{ subject to } d'(I, I_{adv}) \leq \delta, \quad (1)$$

where  $M$  indicates the natural image manifold,  $d$  and  $d'$  denote image distance functions, and  $\delta$  represents the fidelity budget. Through this optimization process, we aim to effectively safeguard images from unauthorized editing and translation while maintaining their fidelity.

### 4 METHOD

In Sec. 4.1, we present the overall framework, followed by details of the Noise Encoder (Sec. 4.2) and the loss function (Sec. 4.3). Sec. 4.4 describes PGD joint optimization, and Sec. 4.5 explains white-box proxy construction for gray-box attacks.

#### 4.1 OVERALL METHOD

This section introduces the overall framework of the Anti-Reference method, as shown in Fig. 2. Our method consists of several key components: the Noise Encoder, a set of conditional modules, the Denoising Unet, and a differentiable data augmentation module. The Noise Encoder adds adversarial noise to the image, forming the protected image  $I_{adv}$ . The set of Reference Modules is a group of conditional control modules that serve as the target models for the attack.

To protect images from the threats posed by tuning-free customization generation methods and driving methods, we selected the pre-trained ReferenceNet from Magic Animate and Econimic, as well as the Stable Diffusion Unet, as the target models for attacking the ReferenceNet route. Additionally, we chose the IP-Adapter as the target model for the Adapter route. The Denoising Unet utilizes the pre-trained Stable Diffusion 1.5 Unet, as it is the most commonly used base model for various customization generation methods. The protected image  $I_{adv}$  is fed into two components: the set of conditional modules and the Denoising Unet, where losses are calculated separately. To enhance the robustness of the adversarial noise against real-world scenarios, we propose a differentiable data augmentation module, which applies common data augmentations to  $I_{adv}$ .

## 4.2 ADVERSARIAL NOISE ENCODER

We propose an adversarial noise encoder (ANE) based on the Vision Transformer (ViT) Dosovitskiy (2020) to efficiently generate adversarial noise in the pixel space, protecting images from threats posed by generative models. The design of the encoder incorporates the following key technical details: ANE adopts the ViT architecture with 12 Transformer layers, a hidden size of 384, and 6 attention heads. The input image is divided into  $8 \times 8$  patches, making it well-suited for detailed feature extraction and adversarial noise predict. The sequence is processed through multiple layers of self-attention and feedforward network modules, resulting in feature vectors. ANE directly generates adversarial noise in the pixel domain instead of relying on latent space.

To enhance robustness, we adopt adversarial training during the training process, including random cropping and scaling, JPEG compression, Gaussian noise, and color transformations. These data augmentation techniques improve the stability of the noise in real-world scenarios, ensuring its effectiveness even after preprocessing or compression. In the training process, to prevent noise from falling into local optima, noise amplitude is regulated through gradient constraints. The model is trained at a resolution of  $512 \times 512$ , maintaining alignment with the common settings of the target generative methods, thereby ensuring compatibility and effectiveness across various generation tasks.

We found that if the conditional model and the denoising Unet shown in Fig. 2 are fixed, ANE tends to generate simple adversarial noise patterns (such as targeting specific vulnerabilities) rather than comprehensively robust noise. This “speculative” behavior may weaken the generator’s generalization ability. To address this, we employ a phased training approach to enhance ANE’s adaptability. In the first phase: the denoising Unet and three kinds of conditional models (IP-Adapter Ye et al. (2023a) and 3 ReferenceNet Chen et al. (2024); Team (2023); Xu et al. (2024) ) are fixed, and ANE is trained to identify effective attack strategies quickly. In the second phase: we randomly perturb the impact weights of the conditional models and switch between different customized models every 1000 steps during training, including replacing the Unet and attaching stylized LoRA Hu et al. (2021) plugins. We obtain these models from the Civitai civ community.

## 4.3 LOSS FUNCTION

**Diffusion Adversarial loss.** In the context of diffusion, in Formula equation 1, which involves maximizing the difference between two images, is transformed into maximizing the difference in noise prediction. Anti-Dreambooth Van Le et al. (2023) was the first to adopt this approach, which was then utilized by subsequent methods Wang et al. (2024a); Ye et al. (2023b); Zheng et al. (2023). This means that we aim for the noise predicted by the model,  $\epsilon_\theta$ , to have the largest possible error compared to the actual noise  $\epsilon$ , thereby disrupting the model’s denoising capability. The specific loss function can be defined as:

$$L_{adv} = -\mathbb{E}_{x_0, \epsilon \sim \mathcal{N}(0, 1), t} [\|\epsilon - \epsilon_\theta(x_t, t)\|^2], \quad (2)$$

where  $x_0$  is the original data,  $\epsilon$  is noise sampled from a standard normal distribution,  $t$  is the time step representing the noise level,  $x_t = \sqrt{\bar{\alpha}_t}x_0 + \sqrt{1 - \bar{\alpha}_t}\epsilon$  is the noisy image at time step  $t$ ,  $\epsilon_\theta(x_t, t)$  is the noise predicted by the model. This loss function is as same as diffusion training loss, but the objective is completely opposite.

**Conditional Adversarial Loss.** Conditional Adversarial Loss aims to attack reference-based customization generation methods and driving techniques. Specifically, we calculate the adversarial noise prediction loss when adversarial noise images are used as inputs for ReferenceNet or IP-adapter. This loss deviates the noise predicted by the denoising Unet from the ground-truth noise, under specific conditional features provided by either ReferenceNet or the IP-adapter. The conditional

adversarial loss is formulated as follows:

$$L_{\text{con\_adv}} = -\mathbb{E}_{x_0, \epsilon \sim \mathcal{N}(0,1), t, c} [\|\epsilon - \epsilon_\theta(x_t, t, c)\|^2], \quad (3)$$

$c$  represents the features extracted from  $I_{\text{adv}}$  using ReferenceNet or IP-adapter. These features interfere with the denoising process by injecting signals into the Unet's cross- or self-attention layers.

**Image Regularization Loss.** To make the adversarial noise less perceptible, we calculate the Mean Squared Error (MSE) of the images before and after noise addition as the regularization loss.

$$L_{\text{reg}} = \text{MSE}(I, I_{\text{adv}}) \quad (4)$$

**Total Loss.** For joint attacks, a weighted loss formulation is employed to ensure a balanced attack performance across various tasks by balancing the impact across all contributions. The total loss, incorporating adversarial, conditional adversarial, and regularization losses, is defined as follows:

$$L_{\text{total}} = w_{\text{adv}} \cdot L_{\text{adv}} + \sum_i w_{\text{con},i} \cdot L_{\text{con\_adv},i} + w_{\text{reg}} \cdot L_{\text{reg}}, \quad (5)$$

where,  $w_{\text{con},i} \cdot L_{\text{con\_adv},i}$  represents the weighted sum of conditional adversarial losses from different conditional modules. Each module  $i$  targets different conditional control tasks, and  $w_{\text{con},i}$  is the specific weight assigned to the conditional adversarial loss for module  $i$ . This paper conducts joint training across four conditional modules: IP-Adapter Ye et al. (2023a), Reference-only Team (2023), Magic Animate Xu et al. (2024), and Ecomimic's ReferenceNet Chen et al. (2024). This approach allows for tailored defenses against a range of adversarial manipulations facilitated by different attack modules, ensuring that the influence of each module is properly scaled according to its significance and effectiveness in the overall defense strategy.

#### 4.4 PGD JOINT OPTIMIZATION

We introduce our Anti-Reference (PGD) method, where adversarial noise is optimized directly using PGD (Projected Gradient Descent). PGD iteratively perturbs the input image  $I$  within a predefined bound, ensuring the noise remains imperceptible while maximizing its impact on the model's predictions. Unlike the Noise Encoder, which generates noise in a single pass, PGD updates the noise iteratively by calculating the gradient of the loss function with respect to the image. At each iteration, the adversarial noise is updated as:

$$I_{\text{adv}}^{(k+1)} = \Pi_{I+\epsilon} \left( I_{\text{adv}}^{(k)} + \alpha \cdot \text{sign} \left( \nabla_{I_{\text{adv}}^{(k)}} L_{\text{total}} \right) \right), \quad (6)$$

where,  $I_{\text{adv}}^{(k)}$  is the adversarial image at iteration  $k$ ,  $\alpha$  is the step size, and  $\epsilon$  defines the perturbation bound. The projection  $\Pi_{I+\epsilon}$  ensures the noise stays within the allowed limits.

By optimizing both  $L_{\text{adv}}$  and  $L_{\text{con\_adv}}$ , PGD effectively disrupts both the diffusion process and conditional adversarial predictions. Our experiments show that PGD provides strong protection across various reference-based customization methods, with gradually increasing noise impact while preserving image quality. Although the Noise Encoder generates noise faster, PGD's iterative process offers stronger protection across tasks at a higher computational cost, making it ideal for scenarios demanding maximum protection.

#### 4.5 GRAY-BOX TRANSFER

This section introduces proxy-based gray-box attacks, a method that generates adversarial samples using a white-box model with a structure similar to the target gray-box model or a closely related latent space. By training DiT to generate adversarial samples on the white-box model, these samples also achieve high attack success rates on the gray-box model. The success of this approach relies on two key factors: 1) structural similarity between the white-box and gray-box models, and 2) shared similarity in their latent spaces. For instance, both Animate Anyone and Magic Animate are based on Stable Diffusion 1.5 and share the same ReferenceNet architecture, with similar datasets used for fine-tuning, resulting in similar latent spaces. Additionally, we successfully attacked the EMO Tian et al. (2024), Animate anyone Hu (2024) and other apps or APIs, as demonstrated in the experiments.

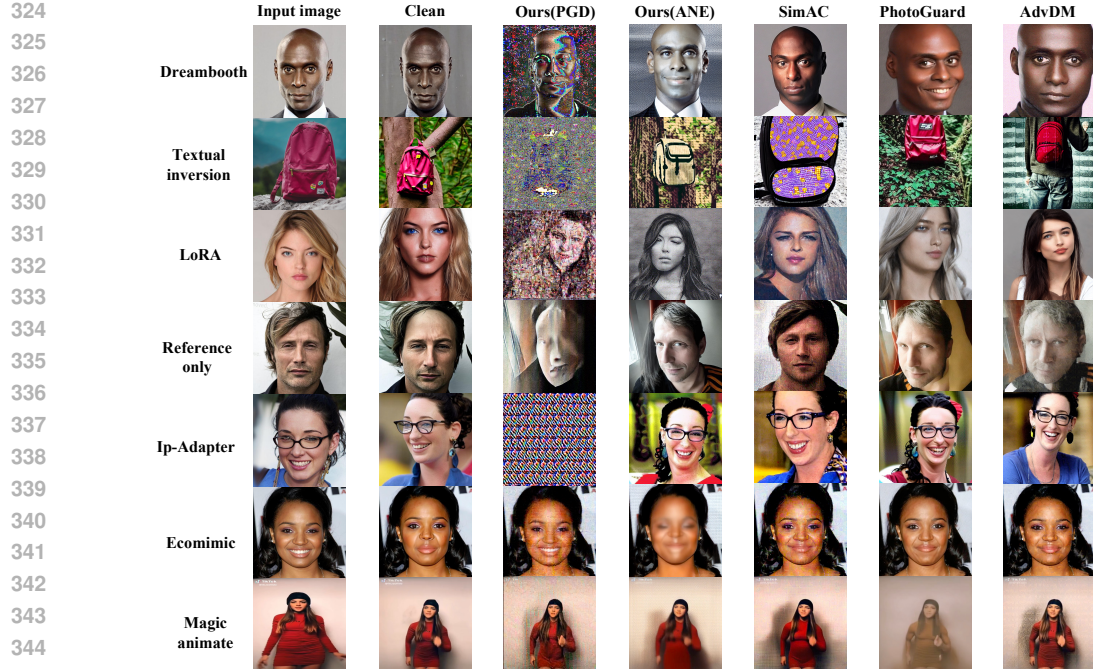


Figure 3: Results of protection methods against customized generation threats. Our approach delivers strong and comprehensive attack performance across scenarios.

## 5 EXPERIMENT

### 5.1 SETUP

**Training data.** This paper aims to achieve general image protection, and therefore, we use 600K natural image-text pairs from the Laion dataset as the training set. To enhance the protection effectiveness for talking face and body-driven tasks, we also include the Celeb-A dataset (200K) and the TikTok dataset (30K) into the training data.

**Experimental details.** We used 4 A100 GPUs to train on 830K image-text pairs for 4 epochs with a batch size of 8, employing a learning rate decay strategy with an initial value of  $10^{-3}$ . We utilized a pre-trained DiT-S/8 model with the same architecture as ANE for the Noise Encoder. During ANE training, adversarial noise is unrestricted; its invisibility is managed by adjusting the weight of image regularization loss. The weights  $w_{\text{adv}}, w_{\text{con1}}, w_{\text{con2}}, w_{\text{con3}}, w_{\text{con4}}, w_{\text{reg}}$  correspond to the fine-tuning attack methods, attacking IP-Adapter Ye et al. (2023a), Reference-only Team (2023), Magic Animate Xu et al. (2024), Ecomimic Chen et al. (2024), and image regularization, respectively. In ANE training, the weights are set to 30, 50, 60, 30, 30, and 200, respectively; in the PGD method, the weights are 3, 5, 5, 2, 2, and 0, respectively.

We implement the Anti-Reference (PGD) method under the following parameter settings. The step size  $\alpha$  is set to  $1 \times 10^{-3}$ , and the number of iterations  $T$  is 300. The perturbation is constrained within an  $\ell_\infty$  norm ball of 0.05, corresponding to a maximum perturbation magnitude of  $\frac{13}{255}$  per pixel. These settings are chosen to balance the attack’s effectiveness and noise invisibility. For more implementation details, please see the supplementary materials.

**Baseline methods.** We use PhotoGuard (Salman et al., 2023), AdvDM (Liang et al., 2023), and SimAC (Wang et al., 2024a) as baselines, with SimAC being an improved version of the classic Anti-DreamBooth (Van Le et al., 2023). We systematically evaluate the protection effectiveness of our method and the baseline methods across seven customization generation tasks, including three fine-tuning-based methods: DreamBooth, LoRA, and Textual Inversion; two tuning-free methods: IP-Adapter and reference-only; and two tasks involving human figure animation: Magic Animate and Ecomimic.

**Evaluation benchmarks.** In constructing the evaluation dataset, we follow previous works. For subject-driven generation, we select 10 subject categories from the DreamBooth dataset Ruiz et al.

(2023), with 3 to 5 images per category. For face-driven tasks, we use 10 identities from the CelebA-HQ dataset. For each subject or individual, we generate a total of 200 images using 10 different prompts for quantitative evaluation. For face-driven and body animation tasks, we generate 200 images using CelebA-HQ and TikTok data, respectively, for quantitative comparison.

**Evaluation metrics.** In our evaluation of person-centric image generation quality, we utilized ISM (Identity Score Matching) metrics (Van Le et al., 2023) to assess protection effectiveness, where lower ISM scores indicate more effective disruption of individual identity in the generated images. Additionally, we measured general image quality using Aesthetics Score (AI, 2023) and CLIP-IQA (CLIP Image Quality Assessment) (Wang et al., 2023), which evaluate the naturalness and perceptual quality of images. These metrics were applied across all frames for tasks involving human body and face-driven content. Lower values in these metrics indicate better image protection effectiveness.

## 5.2 QUANTITATIVE EVALUATION

In this section, we present the quantitative evaluation results and time cost for our method and baselines across seven customized generation methods. For all baseline methods, we use their default code and settings to learn adversarial noise. The results of our two methods used for calculating quantitative metrics are all obtained through joint optimization while results of other baselines are optimized independently on each generation method.

**Critical Oversight.** When training Dreambooth with adversarial images, we followed the common practice of not fine-tuning the CLIP text encoder. The protection performance of Anti-Dreambooth and SimAC relies on the flawed assumption that Bob fine-tunes the CLIP text encoder. See the supplementary materials for details.

Table 1: Quantitative comparison on **ISM Score**.  
Bold values denote best performance.

Method	Ours (PGD)	Ours (ANE)	Sim AC	Adv DM	Photo Guard	Clean
Dreambooth	<b>0.029</b>	0.078	0.051	0.077	0.081	0.287
LoRA	<b>0.005</b>	0.017	0.008	0.015	0.022	0.085
Textual Inversion	<b>0.011</b>	0.123	0.018	0.018	0.304	0.336
IP-Adapter	<b>0.197</b>	0.226	0.225	0.225	0.242	0.233
Reference-only	<b>0.038</b>	0.198	0.096	0.096	0.295	0.348
Echomimic	0.655	<b>0.574</b>	0.673	0.668	0.677	0.715
Magic Animate	0.163	0.221	0.236	0.236	<b>0.134</b>	0.308

Table 2: Quantitative comparison on **Aesthetic Score**. Bold values denote best performance.

Method	Ours (PGD)	Ours (ANE)	Sim AC	Adv DM	Photo Guard	Clean
Dreambooth	<b>5.345</b>	5.716	5.687	5.874	5.935	5.985
LoRA	<b>5.511</b>	5.694	5.719	5.823	5.856	5.951
Textual Inversion	<b>4.344</b>	4.988	4.552	5.400	5.723	5.971
IP-Adapter	<b>5.548</b>	5.930	5.771	6.050	5.961	6.241
Reference-only	<b>4.836</b>	5.480	4.847	5.384	5.996	6.216
Echomimic	5.506	<b>5.370</b>	5.377	5.631	5.461	5.817
Magic Animate	<b>4.451</b>	4.716	5.057	4.988	4.582	4.951

Table 3: Quantitative comparison on **CLIP-IQA**.  
Bold metrics represent methods that rank 1st.

Method	Ours (PGD)	Ours (ANE)	Sim AC	Adv DM	Photo Guard	Clean
Dreambooth	<b>0.550</b>	0.552	0.561	0.631	0.623	0.648
LoRA	<b>0.566</b>	0.579	0.591	0.662	0.634	0.642
Textual Inversion	<b>0.444</b>	0.462	0.500	0.599	0.583	0.653
IP-Adapter	0.445	0.517	0.483	0.566	<b>0.416</b>	0.545
Reference-only	0.584	0.608	<b>0.341</b>	0.523	0.473	0.622
Echomimic	0.419	0.527	<b>0.319</b>	0.573	0.500	0.556
Magic Animate	0.225	0.202	<b>0.184</b>	0.191	0.196	0.217

Table 4: Time Cost of Defense Methods. Our method (ANE) shows a significant advantage.

Method	GPU(s)	CPU(s)
Ours(PGD)	846	-
Ours(ANE)	0.21	1.05
AdvDM	212	-
PhotoGuard	66	-
SimAC	51	-

Table 5: Our method matches SOTA performance in adversarial noise invisibility.

Method	PSNR (↑)	SSIM (↑)
Ours(PGD)	30.39	0.762
Ours(ANE)	29.00	0.713
AdvDM	38.04	0.939
PhotoGuard	32.25	0.822
SimAC	32.17	0.811

**Effectiveness.** From Fig. 3 and Tables 1 to 3, it is evident that our two methods exhibit more comprehensive and thorough attack effects compared to the baseline. Our PGD method effectively protects images from the threats of 7 customized generation methods, and our ANE method also demonstrates effectiveness across all tasks. Specifically, in terms of the most critical ISM metric for measuring the effectiveness of attacks, our method achieved leading results. Our method also holds certain advantages in the Aesthetic-Score and CLIP-IQA metrics.

**Time Cost.** Table 4 shows a comparison of the time required to protect a single image using our method versus the baseline methods. Our method takes only one thousandth of the time required by the baseline methods. This improvement in efficiency marks a crucial advancement from academic research to practical application, laying the foundation for real-world implementation in AI security.

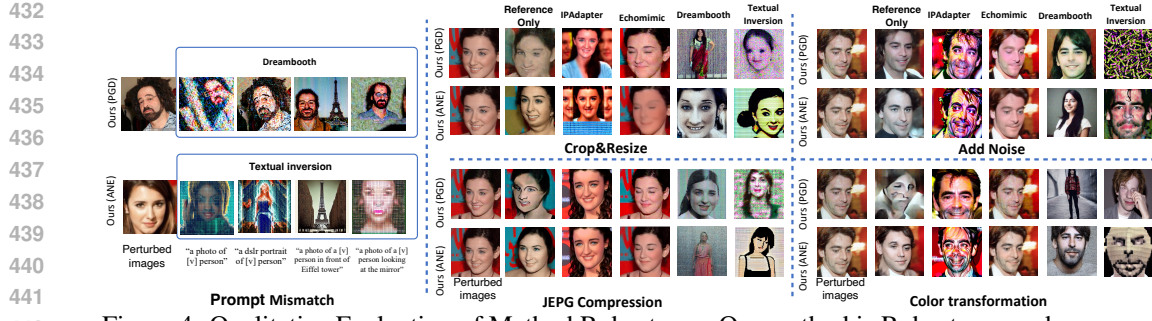


Figure 4: Qualitative Evaluation of Method Robustness. Our method is Robustness under prompt mismatch and image transformation.



Figure 5: Gray-box Attack on Tongyi APIs. Our method successfully compromises both face- and body-driven generation.

**Invisibility.** Table 5 shows a comparison of adversarial noise invisibility. Compared to the baseline, our method produces slightly more noticeable noise, with a trade-off between invisibility and effectiveness. Our approach, which attacks multiple customized generation methods, faces greater convergence challenges than single-task methods, making comparable invisibility difficult to achieve.

### 5.3 GRAY-BOX PERFORMANCE

In this section, we demonstrate the gray-box transferability of our method. We tested the closed-source face-driven method EMO (Tian et al., 2024) and body-driven method Animate Anyone (Hu, 2024) on the Tongyi app ton (2024). Without access to model parameter, our method shows excellent gray-box transferability, with noticeable artifacts in their outputs.

### 5.4 ROBUSTNESS TEST

**Prompt Mismatch.** When Bob customizes concepts with Stable Diffusion, his prompts may differ from Alice’s assumptions during noise generation. PGD-based methods (Van Le et al., 2023), typically trained with fixed prompts (e.g., “a photo of sks person”), suffer under prompt shifts. As shown in Fig. 4, ANE trained on large-scale image-text pairs remains robust to such mismatches.

**Image Transformations.** Our method is robust to common image transformations, such as JPEG compression, crop & resize, noise addition, and color transformations. See supplementary materials for more quantitative results. Our method demonstrates significantly stronger robustness compared to baseline approaches.

## 6 CONCLUSION

This paper introduces Anti-Reference, a novel and effective method for protecting images from the threats posed by mainstream Reference-based generation methods and fine-tuning-based methods. Utilizing a Noise Encoder based on the DiT architecture and a unified loss function, our approach offers universal and efficient protection against various adversarial attacks. Additionally, the introduction of data augmentation techniques and black-box transfer capabilities through white-box proxy models ensures robust and scalable defenses. Extensive experiments validate the effectiveness of Anti-Reference in protecting images from unauthorized customized generation, setting a new standard in the fields of privacy protection and information security.

486    **CODE OF ETHICS**  
487488    The authors have read and acknowledge adherence to the ICLR Code of Ethics.  
489490    **ETHICS STATEMENT**  
491492    All datasets used in this work are publicly available and widely adopted in the research community.  
493    We comply with dataset licenses and usage guidelines. Human figures appear only as part of these  
494    existing benchmarks to evaluate generalization across diverse visual domains. No private or newly  
495    collected human data was used.  
496497    **REPRODUCIBILITY STATEMENT.**  
498500    All datasets, model configurations, and training details used in this work are described in the paper. We  
501    will release the synthetic paired human–robot dataset, model checkpoints, and inference scripts upon  
502    publication to facilitate full reproducibility. Hyperparameters, architecture details, and evaluation  
503    metrics are explicitly documented. We also provide ablation studies to clarify the effect of each  
504    component. Together, these measures ensure that researchers can replicate and extend our results  
505    without ambiguity.  
506507    **USE OF LARGE LANGUAGE MODELS**  
508509    We only used large language models such as GPT-4 and GPT-5 to assist with English grammar  
510    refinement and error correction at the writing stage. All technical content—including method design,  
511    experimental setup, and quantitative results—was independently conceived, implemented, and verified  
512    by the authors. Large language models were not used to modify any experimental data or code. This  
513    guarantees the scientific integrity and originality of this work.  
514  
515  
516  
517  
518  
519  
520  
521  
522  
523  
524  
525  
526  
527  
528  
529  
530  
531  
532  
533  
534  
535  
536  
537  
538  
539

540 REFERENCES  
541

542 Civitai. <https://civitai.com/>. Accessed: 2024-11-15.

543 Tongyi. <https://tongyi.aliyun.com/>, 2024. URL <https://tongyi.aliyun.com/>.  
544 Accessed: 2024-11-15.

545 LAION AI. Aesthetic predictor. <https://github.com/LAION-AI/aesthetic-predictor>, 2023.

546 Tim Brooks, Aleksander Holynski, and Alexei A Efros. Instructpix2pix: Learning to follow image  
547 editing instructions. In Proceedings of the IEEE/CVF Conference on Computer Vision and Pattern  
548 Recognition, pp. 18392–18402, 2023.

549 Xi Chen, Zhiheng Liu, Mengting Chen, Yutong Feng, Yu Liu, Yujun Shen, and Hengshuang  
550 Zhao. Livephoto: Real image animation with text-guided motion control. arXiv preprint  
551 arXiv:2312.02928, 2023.

552 Zhiyuan Chen, Jiajiong Cao, Zhiqian Chen, Yuming Li, and Chenguang Ma. Echomimic: Life-  
553 like audio-driven portrait animations through editable landmark conditions. arXiv preprint  
554 arXiv:2407.08136, 2024.

555 Yunshu Dai, Jianwei Fei, and Fangjun Huang. Idguard: Robust, general, identity-centric poi proactive  
556 defense against face editing abuse. In 2024 IEEE/CVF Conference on Computer Vision and  
557 Pattern Recognition (CVPR), pp. 11934–11943. IEEE, 2024.

558 Jiankang Deng, Jia Guo, Niannan Xue, and Stefanos Zafeiriou. Arcface: Additive angular margin  
559 loss for deep face recognition. In Proceedings of the IEEE/CVF conference on computer vision  
560 and pattern recognition, pp. 4690–4699, 2019.

561 Junhao Dong, Yuan Wang, Jianhuang Lai, and Xiaohua Xie. Restricted black-box adversarial attack  
562 against deepfake face swapping. IEEE Transactions on Information Forensics and Security, 18:  
563 2596–2608, 2023.

564 Alexey Dosovitskiy. An image is worth 16x16 words: Transformers for image recognition at scale.  
565 arXiv preprint arXiv:2010.11929, 2020.

566 Rinon Gal, Yuval Alaluf, Yuval Atzmon, Or Patashnik, Amit H Bermano, Gal Chechik, and Daniel  
567 Cohen-Or. An image is worth one word: Personalizing text-to-image generation using textual  
568 inversion. arXiv preprint arXiv:2208.01618, 2022.

569 Xuanhua He, Quande Liu, Shengju Qian, Xin Wang, Tao Hu, Ke Cao, Keyu Yan, Man Zhou, and  
570 Jie Zhang. Id-animator: Zero-shot identity-preserving human video generation. arXiv preprint  
571 arXiv:2404.15275, 2024.

572 Amir Hertz, Ron Mokady, Jay Tenenbaum, Kfir Aberman, Yael Pritch, and Daniel Cohen-Or. Prompt-  
573 to-prompt image editing with cross attention control. arXiv preprint arXiv:2208.01626, 2022.

574 Jonathan Ho, Ajay Jain, and Pieter Abbeel. Denoising diffusion probabilistic models. Advances in  
575 neural information processing systems, 33:6840–6851, 2020.

576 Edward J Hu, Yelong Shen, Phillip Wallis, Zeyuan Allen-Zhu, Yuanzhi Li, Shean Wang, Lu Wang,  
577 and Weizhu Chen. Lora: Low-rank adaptation of large language models. arXiv preprint  
578 arXiv:2106.09685, 2021.

579 Li Hu. Animate anyone: Consistent and controllable image-to-video synthesis for character animation.  
580 In Proceedings of the IEEE/CVF Conference on Computer Vision and Pattern Recognition, pp.  
581 8153–8163, 2024.

582 Nupur Kumari, Bingliang Zhang, Richard Zhang, Eli Shechtman, and Jun-Yan Zhu. Multi-concept  
583 customization of text-to-image diffusion. In Proceedings of the IEEE/CVF Conference on  
584 Computer Vision and Pattern Recognition, pp. 1931–1941, 2023.

594 Zhen Li, Mingdeng Cao, Xintao Wang, Zhongang Qi, Ming-Ming Cheng, and Ying Shan. Photomaker:  
 595 Customizing realistic human photos via stacked id embedding. In Proceedings of the IEEE/CVF  
 596 Conference on Computer Vision and Pattern Recognition, pp. 8640–8650, 2024.

597

598 Chumeng Liang, Xiaoyu Wu, Yang Hua, Jiaru Zhang, Yiming Xue, Tao Song, Zhengui Xue, Ruhui  
 599 Ma, and Haibing Guan. Adversarial example does good: Preventing painting imitation from  
 600 diffusion models via adversarial examples. arXiv preprint arXiv:2302.04578, 2023.

601 Aleksander Madry. Towards deep learning models resistant to adversarial attacks. arXiv preprint  
 602 arXiv:1706.06083, 2017.

603

604 Zhendong Mao, Mengqi Huang, Fei Ding, Mingcong Liu, Qian He, Xiaojun Chang, and Yongdong  
 605 Zhang. Realcustom++: Representing images as real-word for real-time customization. arXiv  
 606 preprint arXiv:2408.09744, 2024.

607 William Peebles and Saining Xie. Scalable diffusion models with transformers. In Proceedings of  
 608 the IEEE/CVF International Conference on Computer Vision, pp. 4195–4205, 2023.

609

610 Ben Poole, Ajay Jain, Jonathan T Barron, and Ben Mildenhall. Dreamfusion: Text-to-3d using 2d  
 611 diffusion. arXiv preprint arXiv:2209.14988, 2022.

612 Tong Qiao, Bin Zhao, Ran Shi, Meng Han, Mahmoud Hassaballah, Florent Retraint, and Xiangyang  
 613 Luo. Scalable universal adversarial watermark defending against facial forgery. IEEE Transactions  
 614 on Information Forensics and Security, 2024.

615

616 Alec Radford, Jong Wook Kim, Chris Hallacy, Aditya Ramesh, Gabriel Goh, Sandhini Agarwal,  
 617 Girish Sastry, Amanda Askell, Pamela Mishkin, Jack Clark, Gretchen Krueger, and Ilya Sutskever.  
 618 Learning transferable visual models from natural language supervision, 2021.

619

620 Robin Rombach, Andreas Blattmann, Dominik Lorenz, Patrick Esser, and Björn Ommer. High-  
 621 resolution image synthesis with latent diffusion models, 2021.

622

623 Nataniel Ruiz, Yuanzhen Li, Varun Jampani, Yael Pritch, Michael Rubinstein, and Kfir Aber-  
 624 man. Dreambooth: Fine tuning text-to-image diffusion models for subject-driven generation.  
 625 In Proceedings of the IEEE/CVF conference on computer vision and pattern recognition, pp.  
 22500–22510, 2023.

626

627 Hadi Salman, Alaa Khaddaj, Guillaume Leclerc, Andrew Ilyas, and Aleksander Madry. Raising the  
 628 cost of malicious ai-powered image editing. arXiv preprint arXiv:2302.06588, 2023.

629

630 Shawn Shan, Jenna Cryan, Emily Wenger, Haitao Zheng, Rana Hanocka, and Ben Y Zhao. Glaze:  
 631 Protecting artists from style mimicry by {Text-to-Image} models. In 32nd USENIX Security  
Symposium (USENIX Security 23), pp. 2187–2204, 2023.

632

633 Jiaming Song, Chenlin Meng, and Stefano Ermon. Denoising diffusion implicit models. arXiv  
preprint arXiv:2010.02502, 2020.

634

635 Hugging Face Team. Stable diffusion reference implementation, 2023. URL [https://github.com/huggingface/diffusers/blob/main/examples/community/stable\\_diffusion\\_reference.py](https://github.com/huggingface/diffusers/blob/main/examples/community/stable_diffusion_reference.py). Available online.

636

637

638 Linrui Tian, Qi Wang, Bang Zhang, and Liefeng Bo. Emo: Emote portrait alive-generating ex-  
 639 pressive portrait videos with audio2video diffusion model under weak conditions. arXiv preprint  
arXiv:2402.17485, 2024.

640

641 Thanh Van Le, Hao Phung, Thuan Hoang Nguyen, Quan Dao, Ngoc N Tran, and Anh Tran. Anti-  
 642 dreambooth: Protecting users from personalized text-to-image synthesis. In Proceedings of the  
643 IEEE/CVF International Conference on Computer Vision, pp. 2116–2127, 2023.

644

645 Feifei Wang, Zhentao Tan, Tianyi Wei, Yue Wu, and Qidong Huang. Simac: A simple anti-  
 646 customization method for protecting face privacy against text-to-image synthesis of diffusion  
 647 models. In Proceedings of the IEEE/CVF Conference on Computer Vision and Pattern Recognition,  
 pp. 12047–12056, 2024a.

648 Jianyi Wang, Kelvin CK Chan, and Chen Change Loy. Exploring clip for assessing the look and  
 649 feel of images. In Proceedings of the AAAI Conference on Artificial Intelligence, volume 37, pp.  
 650 2555–2563, 2023.

651

652 Qixun Wang, Xu Bai, Haofan Wang, Zekui Qin, and Anthony Chen. Instantid: Zero-shot identity-  
 653 preserving generation in seconds. arXiv preprint arXiv:2401.07519, 2024b.

654

655 Jay Zhangjie Wu, Yixiao Ge, Xintao Wang, Weixian Lei, Yuchao Gu, Wynne Hsu, Ying Shan,  
 656 Xiaohu Qie, and Mike Zheng Shou. Tune-a-video: One-shot tuning of image diffusion models for  
 657 text-to-video generation. arXiv preprint arXiv:2212.11565, 2022.

658

659 You Xie, Hongyi Xu, Guoxian Song, Chao Wang, Yichun Shi, and Linjie Luo. X-portrait: Expressive  
 660 portrait animation with hierarchical motion attention. In ACM SIGGRAPH 2024 Conference  
 661 Papers, pp. 1–11, 2024.

662

663 Zhongcong Xu, Jianfeng Zhang, Jun Hao Liew, Hanshu Yan, Jia-Wei Liu, Chenxu Zhang, Jiashi  
 664 Feng, and Mike Zheng Shou. Magicanimate: Temporally consistent human image animation using  
 665 diffusion model. In Proceedings of the IEEE/CVF Conference on Computer Vision and Pattern  
 666 Recognition, pp. 1481–1490, 2024.

667

668 Hu Ye, Jun Zhang, Sibo Liu, Xiao Han, and Wei Yang. Ip-adapter: Text compatible image prompt  
 669 adapter for text-to-image diffusion models. arXiv preprint arXiv:2308.06721, 2023a.

670

671 Xiaoyu Ye, Hao Huang, Jiaqi An, and Yongtao Wang. Duaw: Data-free universal adversarial  
 672 watermark against stable diffusion customization. arXiv preprint arXiv:2308.09889, 2023b.

673

674 Shiwei Zhang, Jiayu Wang, Yingya Zhang, Kang Zhao, Hangjie Yuan, Zhiwu Qin, Xiang Wang, Deli  
 675 Zhao, and Jingren Zhou. I2vgen-xl: High-quality image-to-video synthesis via cascaded diffusion  
 676 models. arXiv preprint arXiv:2311.04145, 2023.

677

678 Yuxuan Zhang, Yiren Song, Jiaming Liu, Rui Wang, Jinpeng Yu, Hao Tang, Huaxia Li, Xu Tang,  
 679 Yao Hu, Han Pan, et al. Ssr-encoder: Encoding selective subject representation for subject-  
 680 driven generation. In Proceedings of the IEEE/CVF Conference on Computer Vision and Pattern  
 681 Recognition, pp. 8069–8078, 2024a.

682

683 Yuxuan Zhang, Lifu Wei, Qing Zhang, Yiren Song, Jiaming Liu, Huaxia Li, Xu Tang, Yao Hu, and  
 684 Haibo Zhao. Stable-makeup: When real-world makeup transfer meets diffusion model. arXiv  
 685 preprint arXiv:2403.07764, 2024b.

686

687

688 Yuxuan Zhang, Qing Zhang, Yiren Song, and Jiaming Liu. Stable-hair: Real-world hair transfer via  
 689 diffusion model. arXiv preprint arXiv:2407.14078, 2024c.

690

691 Boyang Zheng, Chumeng Liang, Xiaoyu Wu, and Yan Liu. Understanding and improving adversarial  
 692 attacks on latent diffusion model. arXiv preprint arXiv:2310.04687, 2023.

693

694

695

696

697

698

699

700

701

## SUPPLEMENTARY MATERIALS OF "ANTI-REFERENCE: UNIVERSAL AND IMMEDIATE DEFENSE AGAINST REFERENCE-BASED GENERATION"

## A CRITICAL OVERSIGHT

It is worth noting that when training Dreambooth with adversarial images, we did not fine-tune the CLIP text encoder, which aligns with the common practice in the community. We found that the good protection performance of Anti-Dreambooth and SimAC is based on the incorrect assumption that Bob will fine-tune the CLIP text encoder. As shown in Figure 6, when Bob does not fine-tune the CLIP text encoder during Dreambooth training, both of these image protection methods show a significant drop in performance, regardless of whether the CLIP text encoder was fine-tuned during the noise learning process. Our method does not suffer from this issue.

		Does Alice fine-tune the text encoder ?	
		True	False
			
Clean images	 	True	False
Does Bob fine-tune the text encoder ?		True	False
	 	 	 

Figure 6: We have identified a critical oversight in the current SimAC method; when Bob does not train the Text Encoder while training Dreambooth, the protection effectiveness of the images is significantly compromised.

## B DETAIL OF EVALUATION METRICS

For evaluating the quality of person-centric image generation, we used widely adopted metrics ISM (Van Le et al., 2023) to quantify the generation quality, where lower ISM represent better protection effectiveness. Additionally, we employed two general image quality assessment metrics, Aesthetic Score (AI, 2023) and CLIP-IQA (Wang et al., 2023). For human body and face-driven tasks, we calculated quantitative metrics across all frames.

- **ISM (Identity Score Matching):** Measures the cosine similarity between the features of the generated face and the original face to evaluate how well the generated image maintains the identity of the subject.
- **Aesthetic Score:** An aesthetic assessment metric that utilizes a linear estimator built on top of CLIP to predict the aesthetic quality of images.
- **CLIP-IQA (CLIP Image Quality Assessment):** Uses CLIP (Contrastive Language-Image Pretraining) to evaluate the perceptual quality of images by assessing how well the visual features of the image align with text descriptions.

## C TRANSFERABILITY OF ADVERSARIAL NOISE ACROSS MODEL ARCHITECTURES

Due to the architectural differences among SD1.5, SD2.0, and SD-XL, their latent spaces significantly differ. We have conducted experiments with adversarial noise on SD1.5, but it could not be generalized to SD-XL. This issue is not unique to our method; there are no successful transfer precedents in this field. Table. 6 shows the transferability results for Anti-Reference, where noise can be transferred

756 between SD1.4 and SD1.5 due to their similar architectures and latent spaces. We perform a joint  
 757 attack across models with different architectures, and experimental results show that this strategy  
 758 effectively enables simultaneous attacks on methods with varying backbones.

760 Table 6: Transferability results of adversarial attacks across different SD architectures.  
 761

762 <b>Attack</b>	763 <b>SD1.4</b>	764 <b>SD1.5</b>	765 <b>SD2.0</b>	766 <b>SD-XL</b>
767 SD1.5	✓	✓	✗	✗
768 SD2.0	✗	✗	✓	✗
769 SD-XL	✗	✗	✗	✓
770 Joint attack on SD1.5, 2.0, XL	✓	✓	✓	✓

771 

## D HUMAN EVALUATION

772 To further validate the effectiveness of our proposed methods in perceptual scenarios, we conducted  
 773 a human evaluation study via an online questionnaire. Participants were presented with a series of  
 774 images generated by different models using both clean and adversarial inputs. They were asked to  
 775 determine whether each image exhibited visible artifacts or distortions. All images were presented in  
 776 randomized order, and participants were not informed which ones contained adversarial perturbations  
 777 to minimize bias.

778 A total of 30 participants took part in the evaluation, each reviewing 50 image samples. For each  
 779 image, they were instructed to answer two questions: (1) whether the image contained visible artifacts,  
 780 and (2) whether it exhibited noticeable distortions. The evaluated samples included adversarial images  
 781 generated by our two proposed methods: PGD (Projected Gradient Descent) and ANE (Adversarial  
 782 Noise Embedding).

783 As shown in Tab. 7, the results demonstrate that the PGD method is highly effective at introducing  
 784 perceptible artifacts. Meanwhile, our ANE method also achieves strong perceptual impact, producing  
 785 noticeable distortions in the generated images. Both methods successfully mislead the generation  
 786 models while being perceptible to human observers, highlighting their practical utility and robustness  
 787 in adversarial attack settings.

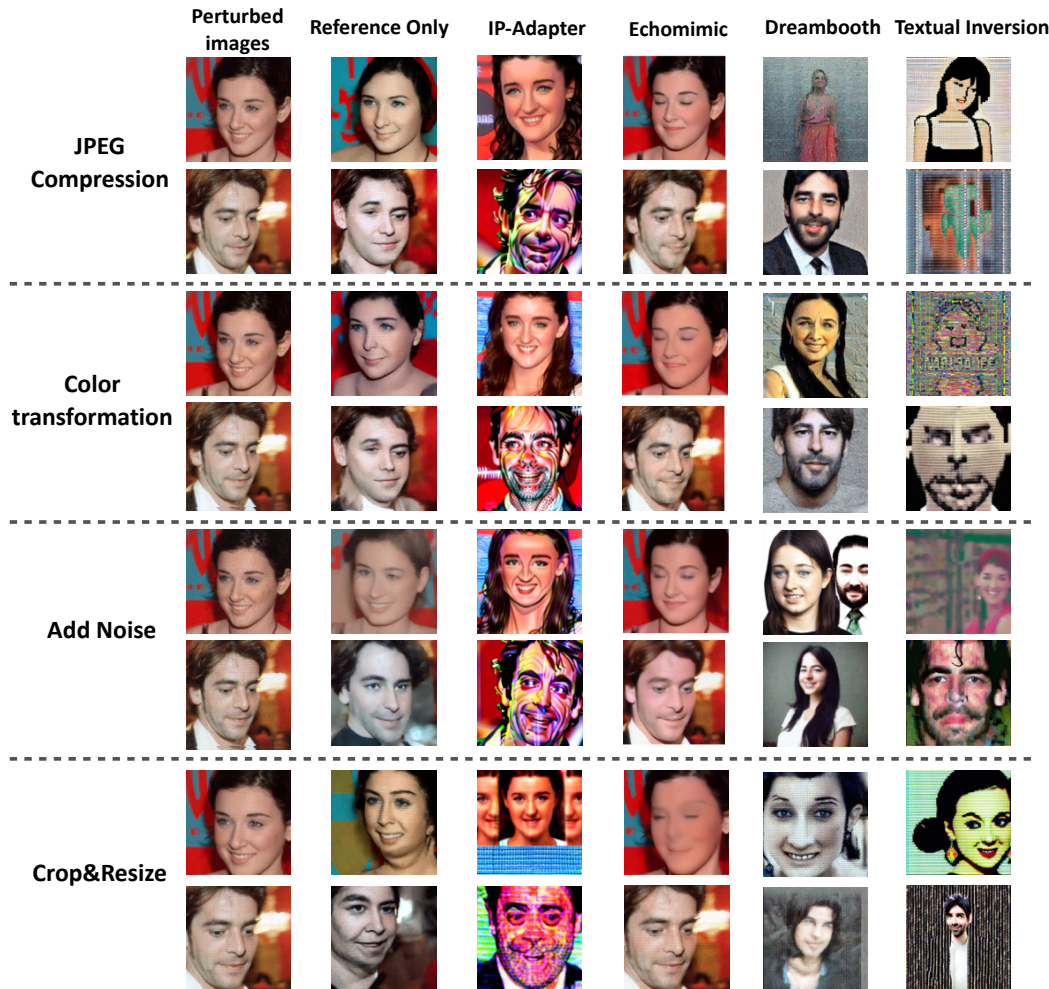
788 Table 7: Percentage of users judging the attack as successful (obvious artifacts observed). Bold  
 789 metrics indicate top-ranked methods.

790 Method	791 Ours(PGD)	792 Ours(ANE)	793 SimAC	794 AdvDM	795 PhotoGuard
796 Dreambooth	<b>100</b>	<b>100</b>	93	85	90
797 LoRA	<b>97</b>	92	94	69	93
798 Textual Inversion	<b>100</b>	<b>100</b>	96	85	89
799 IP-Adapter	<b>93</b>	89	72	65	67
800 Reference-only	<b>96</b>	94	<b>96</b>	87	93
801 Echomimic	<b>100</b>	<b>100</b>	<b>100</b>	94	98
802 Magic Animate	<b>100</b>	<b>100</b>	<b>100</b>	<b>100</b>	<b>100</b>

803 

## E LIMITATIONS AND FUTURE WORK

804 While our method inherits the common challenge of imperceptible adversarial cues—shared by most  
 805 SOTA defenses—it remains effective in disrupting generation outputs across models. Our approach  
 806 is built on SD 1.5 to align with widely-used reference-based generation systems, with results on  
 807 SD-XL and SD3 included in the supplementary. Future work will extend compatibility to emerging  
 808 architectures such as Diffusion Transformers.

810 F MORE ROBUSTNESS TEST RESULTS  
811812 Figure 7 and 8 shows that our method is robust to common image transformations, such as JPEG  
813 compression, crop & resize, noise addition, and color transformations.  
814847 Figure 7: More robustness test results: Our method (ANE) is robust against common image transfor-  
848 mations.

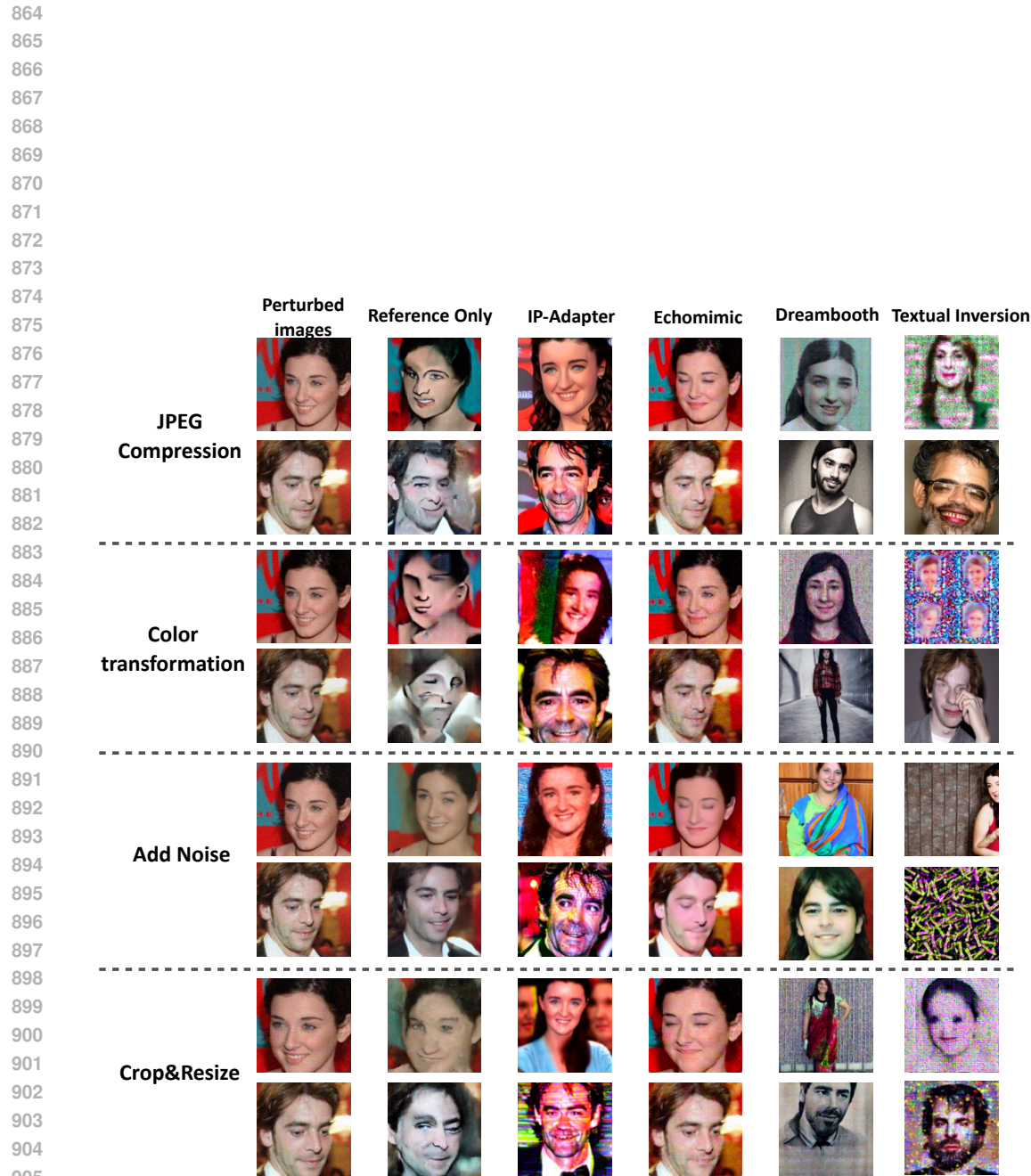


Figure 8: More robustness test results: Our method (PGD) is robust against common image transformations.